Journal of Oceanology and Limnology
Vol. 38 No. 2, P. 334-341, 2020
https://doi.org/10.1007/s00343-019-9102-0

Influence of simulating deep-sea environmental factors on cathodic performance of seawater battery*

LU Yonghong[1], YANG Lulu[1], ZHANG Yue[1], ZHAO Qing[2], SANG Lin[2], DING Fei[2], XU Haibo[1, **]

[1] *College of Chemistry and Chemical Engineering, Ocean University of China, Qingdao 266100, China*

[2] *National Key Laboratory of Science and Technology on Power Sources, Tianjin Institute of Power Sources, Tianjin 300084, China*

Received Apr. 15, 2019; accepted in principle May 20, 2019; accepted for publication May 24, 2019

Abstract A metal-dissolved oxygen seawater battery (SWB) uses metal and dissolved oxygen as the reactants, and it is ideal for use as a long-time low-power distributed power supply in deep sea, due to its advantages of open structure in service without electrolyte. However, several simulating deep-sea environmental factors, such as flow rate, dissolved oxygen concentration, and temperature of seawater may affect the oxygen reduction reaction (ORR) rate and the stability of electrochemically modified polyacrylonitrile-based carbon fiber brush (MPAN-CFB) cathode, which was studied by steady-state polarization and galvanostatic discharge methods. In addition, the scales formed on MPAN-CFB surface were characterized by SEM and XRD. Results show that the ORR rate increased quickly with the increase of the seawater flow rate up to 3 cm/s, and then gradually stabilized. Moreover, the ORR rate was largely affected by dissolved oxygen concentration, and the concentration of >3 mg/L was favorable. Compared with surface layer temperature of 15°C, the low temperature of deep sea (4°C) has a negligible effect on ORR rate. When the working current is too high, it will lead to the formation of $CaCO_3$ scales (aragonite) of at the cathodic surface, resulting in the decrease of ORR rate, and consequently the damage to the long-time stability of MPAN-CFB.

Keyword: seawater battery (SWB); deep sea; modified polyacrylonitrile-based carbon fiber brush (MPAN-CFB); oxygen reduction reaction (ORR); scale formation

1 INTRODUCTION

Cathodic reaction of a metal-dissolved oxygen seawater battery (a simple abbreviation as SWB) depends mainly on the reduction of dissolved oxygen in seawater to obtain the electron (oxygen reduction reaction (ORR), Eq.1), while the anodic reaction of SWB depends on metals with high negative potential, such as magnesium (Mg) alloy (Eq.2), to dissolute and donate the electron, and the seawater is used as electrolyte, whose ocean current can transport oxygen and eliminate by-products—$Mg(OH)_2$ and $CaCO_3$ (Eqs.3 and 4) (Song and Wang, 2004; Sun et al., 2008). In fact, as a no-pollution and renewable marine distributed power source, SWB is usually designed as an open structure to safely put into use without pressure-resistant cabin, and it has been confirmed that the ultrahigh pressure of 1 100 bar under simulated deep sea condition brings negligible effects on the performance of battery and electrodes (Liu et al., 2017). Moreover, SWB has high energy density of 700–1 200 Wh/kg which is determined by the anodic performance, thus it is suitable as the long-term power supply in years for low-power deep-sea observation equipment (such as submarine geology exploration, underwater acoustic communication, navigation and early-warning information platform, etc.), so as to avoid using expensive and unsafe submarine cable or hundreds of kilograms to tons weighted primary lithium battery (Xu et al., 2012; Hahn et al., 2015).

* Supported by the National Major Scientific Instruments Development Project of the National Natural Science Foundation of China (No. 41427803) and the Zhuang Fa Yu Yan Program (No. 41421020401)

** Corresponding author: xuwangri@163.com

In addition, the power density of SWB is determined by the cathodic performance, and the improvement of cathodic ORR catalytic activity is always a hot topic in electrochemical fields (Guo et al., 2016; Liu et al., 2016). At present, the commonly-used cathodic materials are carbon fiber, graphite, stainless steel, copper and air electrodes, and so on, in which the carbon fiber has the advantages of corrosion resistance, large surface area, excellent flexibility, good electrical conductivity and stability (Hasvold, 1990; Hasvold et al., 1997; Wang et al., 1997; Wilcock and Kauffman, 1997; Shinohara et al., 2009). SWB has been commercialized at present. In 2009, Japan used SWB1200 (a product of assembling carbon fiber with magnesium alloy from Kongsberg Simrad, Norway) for a sea floor seismic observatory at 5 577-m water depth for >5 years, but the volume specific power is only 2.7 mW/L due to a poor cathodic activity (Shinohara et al., 2009; Jiao et al., 2018). On that basis, the commercial polyacrylonitrile-based carbon fiber (PAN-CF) was made into the brush electrode, and then it was electrochemically modified to convert its inherent pyridinic-N into 2-pyridone (or 2-hydroxyl pyridine) functional group with remarkable ORR catalytic activity (Xu et al., 2015). The modified PAN-CF brush electrode (denoted as MPAN-CFB) was used in a real sea test by combining with Mg alloy to fabricate into Mg-dissolved oxygen SWB, whose high electrocatalytic activity and stability have also been successfully confirmed (Xu et al., 2012, 2015).

However in real sea application, SWB performance was observed not only to depend on the activity and stability of cathodic material itself, but also to be closely related to the marine environment. Concerned with deep sea, some factors, e.g. flow rate (2–15 cm/s), dissolved oxygen concentration (0–6 mg/L) and temperature (0–4°C) etc., directly or indirectly affect the cathodic reaction rate (Chen, 2009; Xu et al., 2012). In particular, the flow rate and dissolved oxygen concentration determine the supply speed and amount of oxygen to cathodic surface, and the temperature also affects the reaction rate directly (Zha, 2002).

In addition, these factors influence the scale formation on SWB cathodic surface. This process is similar to that arising from hydrogen evolution reaction (HER, Eq.5) in corrosion-resistant cathodic protection (CP) of steel; however the former disturbs the oxygen transfer and gives damage to SWB performance, whereas the latter does favor to metal anti-corrosion against aggressive medium (Neville and Morizot, 2002; Morse et al., 2007). Particularly, both ORR and HER produce OH^- and cause the surface alkalization on cathodic surface, which probably result in the formation of scale layer, including aragonite and calcite precipitation of $CaCO_3$, and brucite of $Mg(OH)_2$, etc. (Mucci, 1983). Meanwhile, the ocean convection affects the degree of alkalization, which possibly takes away some or even all of the precipitates to weaken the scaling tendency, if only the seawater flow rate is large enough. Moreover, the low temperature in deep sea increases the solubility product of $CaCO_3$, decreases the precipitation rate of the scales, or even changes their polymorph, e.g. aragonite or calcite (Mucci, 1983; Morse et al., 2007).

At present, many references focus on how marine environmental parameters and working current/voltage affect the scale formation on metal surface under CP, whereas few relates them with the ORR rate and scaling tendency of carbon-based materials. Therefore, by point-by-point steady-state polarization and galvanostatic test (i.e. constant-current discharge) method, the influences of flow rate, temperature and dissolved oxygen concentration of seawater on MPAN-CFB performance of SWB are investigated in simulating deep-sea environment, and the scales are characterized by SEM and XRD to determine the morphology and composition, in order to promote the SWB deep-sea application in resource exploration and safety guarantee early.

Cathodic reaction (ORR):

$$O_2+2H_2O+4e\rightarrow 4OH^-. \quad (1)$$

Anodic reaction:

$$Mg\rightarrow Mg^{2+}+2e. \quad (2)$$

Side reactions:

$$Mg^{2+}+2OH^-\rightarrow Mg(OH)_2, \quad (3)$$

$$Ca^{2+}+HCO_3^-+OH^-\rightarrow CaCO_3+H_2O. \quad (4)$$

Cathodic reaction (HER):

$$2H_2O+2e\rightarrow 2OH^-+H_2. \quad (5)$$

2 MATERIAL AND METHOD

2.1 Brush electrode preparation and activation

An amount of 6.32 g PAN-CF wire beam (Toray T700SC/24K, ~7 μm fiber diameter, 1.65 g/m linear density) is made into brush electrode (18 cm length, 7 cm body diameter) with titanium wire (TA2, 1.5 mm diameter). PAN-CFB is modified in 2 mol/L H_2SO_4 solution by recurrent galvanic pulse method, i.e.

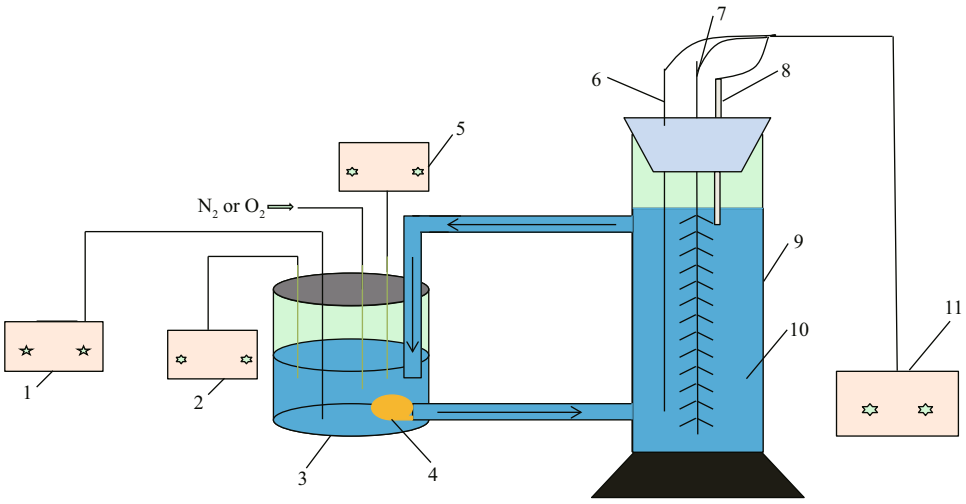

Fig.1 Diagram of simulating experimental device

1: power supply; 2: dissolved oxygen meter; 3: storage tank; 4: water pump; 5: pH meter; 6: auxiliary electrode; 7: working electrode; 8: reference electrode; 9: reaction tank; 10: temperature-controlled seawater; 11: potentiostat/galvanostat.

cycling 6 times from 5.0 A anodic current for 300 s to the same cathodic current for 300 s, and then stabilized at 1.4 V for 1 h to prepare MPAN-CFB.

2.2 Experimental device and electrochemical test

The simulating experimental device is shown in Fig.1. The temperature of natural seawater (pH 8.2, Qingdao Jiaozhou bay) was controlled by a constant- and low-temperature cooling tank (YT-DW-2B, Wuhan Yite Instrument Co. Ltd., China). A DC submerged water pump placed in an enclosed 5-L liquid storage tank was used to circulate the seawater between storage tank and reaction tank and regulate the flow rate. N_2 or O_2 from gas bottle was input into liquid storage tank to adjust the dissolved oxygen concentration in seawater, which was monitored in real time by a dissolved oxygen meter (JPSJ-605, Shanghai Leici Instrument Factory, China). The value of pH was monitored by a Model pH meter (E-201-C, Shanghai Leici Instrument Factory, China).

Conventional three-electrode systems in enclosed reaction tank was used, MPAN-CFB as working electrode, a self-made Ti/IrO_2 mesh plate as auxiliary electrode and a saturated calomel electrode (SCE) as reference electrode. A potentiostat/galvanostat (ZF-9, Shanghai Zhengfang Electronics Co. Ltd., China) was used and all potentials are referred to the SCE.

Steady-state polarization curves were tested in the range of -700–50 mV, changing the potential every 50–100 mV and recording the current after 3 min stabilization under these conditions: room temperature of 15°C or low temperature of 4°C, 9 mg/L saturated oxygen concentration or 1–6 mg/L dissolved oxygen concentration, and 1–6 cm/s seawater flow rate. The galvanostatic discharge curves of MPAN-CFB at different current (-100, -200, and -300 mA) were tested in 15°C, naturally aerated seawater with 2 cm/s flow rate. After working for some time, MPAN-CFB was taken out and immerged into 0.1 mol/L HCl solution to remove the by-products. After physical characterization, the discharge tests proceeded again.

2.3 Physical characterization

The morphology of MPAN-CFB before and after -300 mA galvanostatic discharge was observed by scanning electron microscopy (SEM; TM-1000, Hitachi) with an accelerating voltage of 10 kV, and its X-ray diffraction (XRD) pattern after discharge test was measured by using a Cu Kα radiation system (40 kV, 100 mA, 6/min, D8 Advance, Bruker).

3 RESULT AND DISCUSSION

3.1 Effect of flow rate on MPAN-CFB performance

Photos of cathode before and after modification are shown in Fig.2. It can be seen that before modification (the left), the PAN-CFB cathode shows typical gray-black metallic luster of carbon fiber; while after modification (the right), the MPAN-CFB cathode looks blacker or even colorful under sunshine due to light scattering.

Polarization curves of PAN-CFB (Fig.3a) and MPAN-CFB (Fig.3b) were compared in seawater (15°C, 9 mg/L saturated oxygen concentration) with different flow rate. It can be seen that the ORR activity of MPAN-CFB was greatly improved. A positive shift

of the initial oxygen reduction potential (E_{onset}) from -250 mV to -50 mV occurred. At the same time, the ORR current density of MPAN-CFB was increased by 6–27 times compared with that of PAN-CFB at different polarization potential. For example, under a 3 cm/s seawater flow rate, the ORR current density of MPAN-CFB reached -178.9 mA/g, whereas that of PAN-CFB was only -6.5 mA/g at -450 mV.

Moreover, the seawater flow rate significantly affected the ORR rate. The current density of both PAN-CFB and MPAN-CFB was very low at 1 cm/s, owing to a much higher consuming rate of dissolved oxygen than its supply rate on electrode surface. As we know, at a low flow rate, the mass transfer of dissolved oxygen mainly relies on natural diffusion, so that the ORR rate was controlled by the diffusion process and thereby showed low reaction activity. At 2 cm/s, the current density was significantly increased; but from 3 cm/s on, its rising tendency slowed down, corresponding to the previous conclusions that the commercial SWB needs to be used at >2 cm/s seawater flow rate, in order to guarantee a good ORR catalytic effect and satisfy the performance requirement of SWB for a long-range, autonomous underwater vehicle (Hasvold et al., 2004). Therefore, a value of 3 cm/s indicates a critical seawater flow rate for SWB.

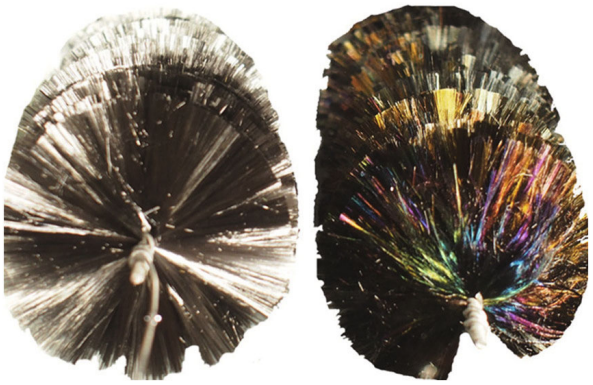

Fig.2 Morphology of SWB cathode before (left) and after (right) modification

3.2 Effect of dissolved oxygen concentration on MPAN-CFB performance

Steady-state polarization curves (E-Log$I$) of MPAN-CFB in seawater (15°C, a slow flow rate of 2 cm/s) with 1–6 mg/L oxygen concentration are displayed in Fig.4. We divide the curves into two parts: zone I of -50– -250 mV (low current density) where the ORR was controlled by typical electrochemical process and diffusion process simultaneously; and zone II of -250– -700 mV (high current density) where the ORR was solely controlled by oxygen diffusion process. No matter in zone I or II, the reaction rate on MPAN-CFB was greatly affected by the dissolved oxygen concentration, especially at <3 mg/L. Considering an open structure of SWB, several SWBs must be used in parallel other than in series to prevent the power supply loss from solution resistance, which resorted to the DC-DC voltage booster to enhance the output voltage to a higher value (e.g. to 24 V or 36 V). Therefore, the cathodic ORR process of SWB was usually kept in zone I, in order to provide a >1.2-V output voltage, due to the restriction of voltage-boosting efficiency (the higher output voltage gives, the higher voltage-boosting

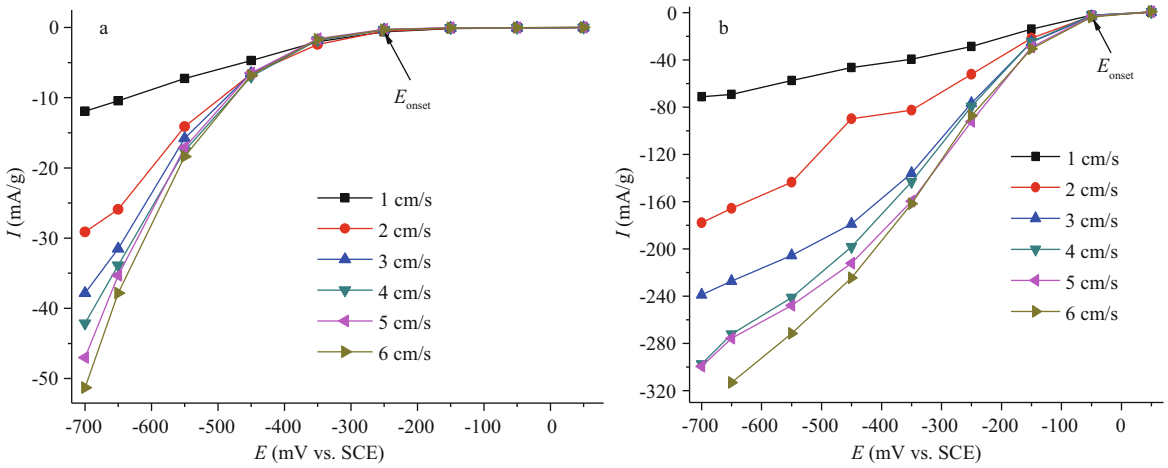

Fig.3 Effect of seawater flow rate on SWB cathodic performance

Seawater condition: 15°C, 9 mg/L dissolved oxygen concentration, 1–6 cm/s flow rate. a. polarization curves of PAN-CFB; and b. polarization curves of MPAN-CFB. E_{onset} in graphs represents the initial oxygen reduction potential.

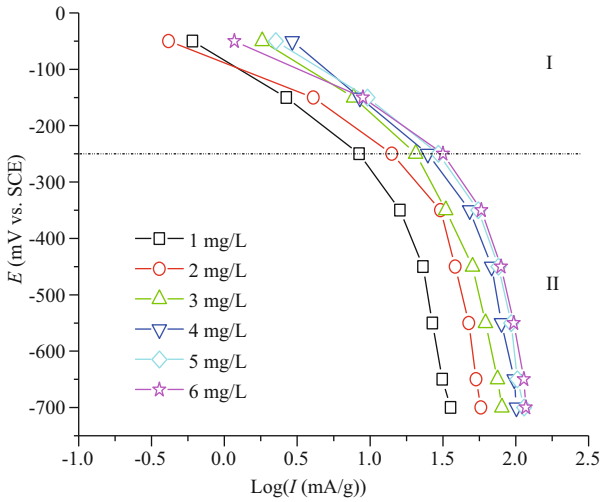

Fig.4 Effect of seawater oxygen concentration on SWB cathodic performance

E-Log*I* curves of MPAN-CFB in seawater (15°C, 2 cm/s flow rate, 1–6 mg/L dissolved oxygen concentration). The curves are divided into two section: zone I (low current density) and zone II (high current density).

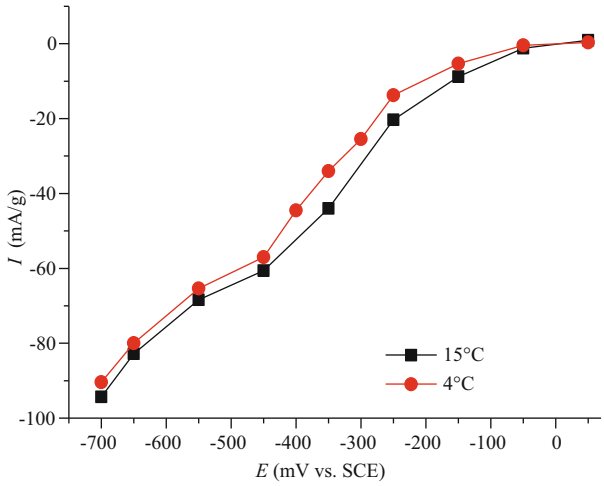

Fig.5 Effect of seawater temperature on SWB cathodic performance

Polarization curves of MPAN-CFB in seawater (4 cm/s flow rate, 3 mg/L dissolved oxygen concentration, 4°C or 15°C).

efficiency achieves). From the polarization curve of zone I, the difference in current density seemed small once the dissolved oxygen concentration reached >3 mg/L. Therefore, a favorable oxygen concentration of >3 mg/L is required for high SWB performance in deep sea.

3.3 Effect of temperature on MPAN-CFB performance

Steady-state polarization curves of MPAN-CFB in seawater (4 cm/s flow rate, 3 mg/L oxygen concentration) at simulated deep-sea low temperature of 4°C and

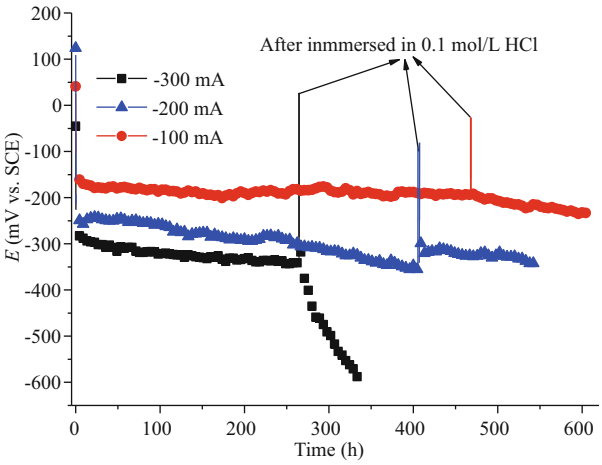

Fig.6 Long-term stability test of SWB cathodic performance

Galvanostatic discharge curves of MPAN-CFB in naturally aerated seawater (15°C, 2 cm/s flow rate), and after 466 h at -100 mA, 400 h at -200 mA and 260 h at -300 mA, it is taken out and immerged into 0.1 mol/L HCl to remove the by-products, and then continue the discharge test again.

marine surface temperature of 15°C are compared in Fig.5. It can be observed that both curves are approximately similar in shape, indicative of the same reaction mechanism and the controlled process. Two curves start at nearly the same E_{onset}; the cathodic current density increases with a negative shift of polarization potential from -50 mV to -700 mV, and the difference in current density reaches 10 mA/g at -350 mV at first but then reduces to 3 mA/g from -450 mV on, i.e. a more decrease of ORR rate at low cathodic potential. The influence of low temperature on chemical reaction rate lies in a decrease of mass transfer and an increase of solution resistance, which can be observed in Fig.5 clearly. It indicates that the temperature had a little effect on ORR rate, which is often neglected in marine engineering considering its allowable error.

3.4 Long-term stability test

Galvanostatic discharge tests at -100 mA, -200 mA and -300 mA were performed in naturally aerated seawater (15°C, 2 cm/s flow rate), to investigate the long-term stability of MPAN-CFB (Fig.6). During the whole experiments, the pH value of seawater changed very little. It can be seen that the polarization potential decreased largely with the time at -200 mA and -300 mA, a drop of 120 mV in 400 h and 100 mV in 260 h, respectively, but only 20 mV in 466 h at -100 mA. Considering the initial pH 8.2 of the sample seawater, together with the OH^- accumulation from ORR process, they easily led to the surface alkalization combiningly and form the $CaCO_3$ scale layer on

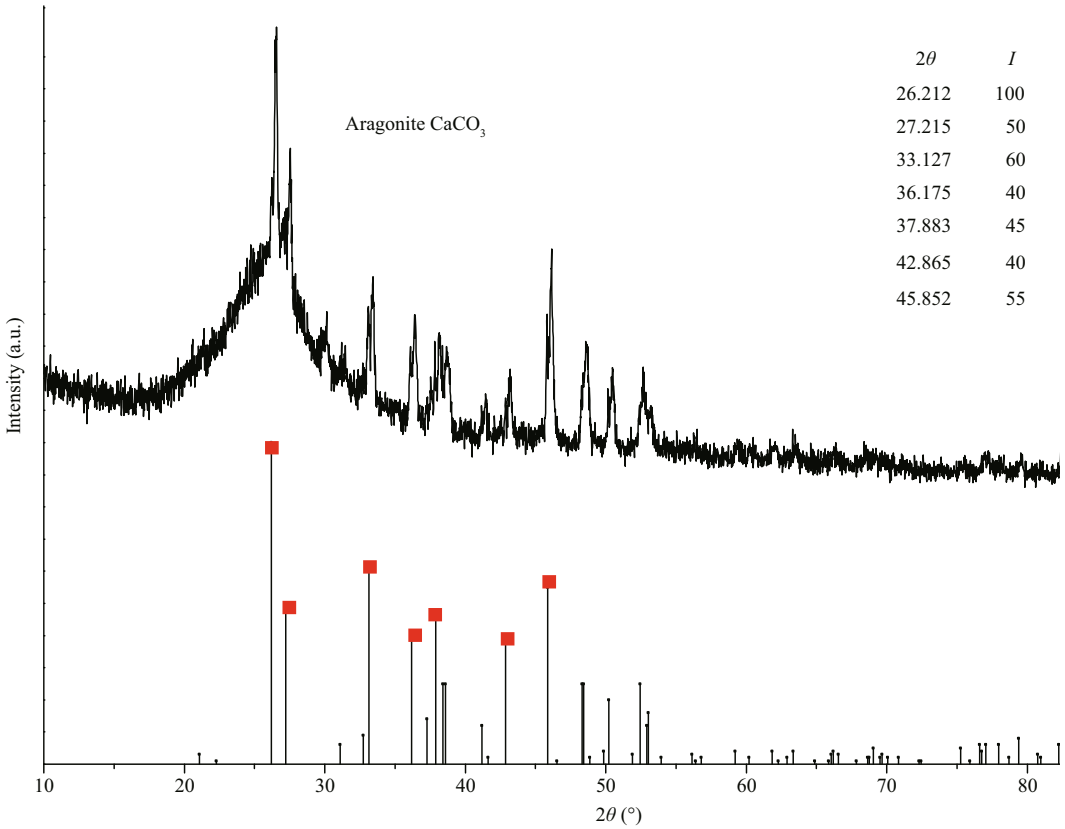

Fig.7 Scale composition on SWB cathode by XRD

After 260 h galvanostatic discharge test at -300 mA, MPAN-CFB surface is characterized to determine the composition.

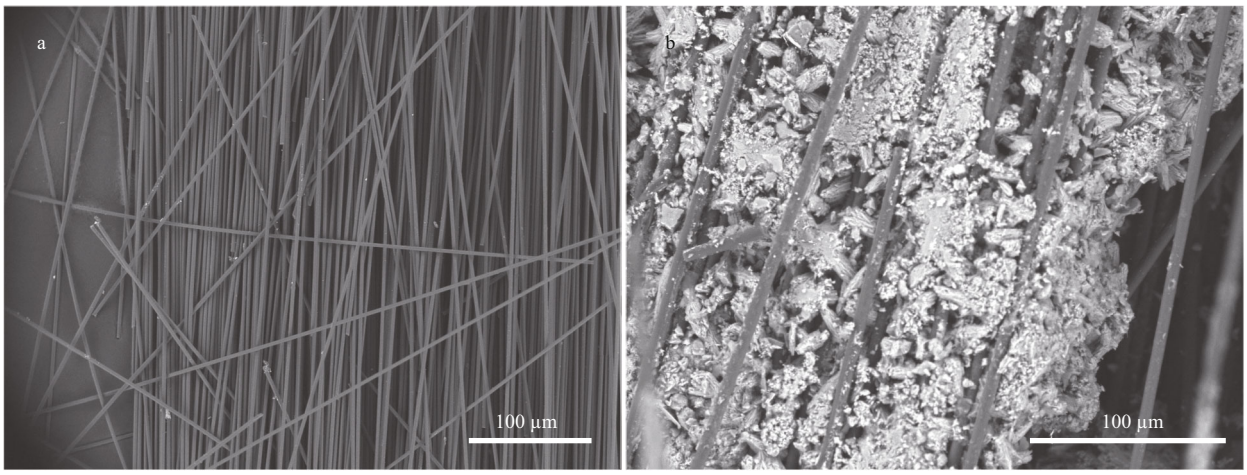

Fig.8 Surface morphology on SWB cathode by SEM

a. original MPAN-CFB; b. MPAN-CFB after 260 h galvanostatic discharge test at -300 mA.

MPAN-CFB surface ($Mg(OH)_2$ usually produces at higher temperature and pH), which may hinder the mass transfer of oxygen, and negatively give rise to a large shift of polarization potential, especially at high working current.

And then, to verify the composition of scales, the working MPAN-CFBs were taken out to immerse into 0.1 mol/L HCl solution, and many bubbles were found, preliminarily indicative of the appearing of CO_2 from $CaCO_3$. At the same time, they were characterized by XRD (Fig.7), and the $CaCO_3$ with aragonite structure was confirmed. Some fiber wires were taken from MPAN-CFB at -300 mA to be characterized by SEM (Fig.8). Compared with the

blank sample before galvanostatic discharge (Fig.8a), it can be seen that many sediments accumulateed to form a compact scale layer on MPAN-CFB surface (Fig.8b).

For calcareous deposit on carbon steel under CP, $Mg(OH)_2$ deposit did not appear until pH>9.7 (Barchiche et al., 2003). Under natural corrosion of low carbon steel in seawater whose cathodic process usually belongs to the ORR, the compact aragonite was more likely formed than calcite of $CaCO_3$ with the influence of Mg^{2+}, which largely retarded the oxygen diffusion consequently (Möller, 2007).

Finally, after immersed in HCl for half an hour, the MPAN-CFBs were rinsed to neutral pH and then continue the galvanostatic experiment. The results are shown in the latter half of Fig.6. We can see that the performance of MPAN-CFB at -100 mA and -200 mA was almost recovered, but that at -300 mA did not. Some structure damages to MPAN-CFB might occur after HCl immersion and thus the cathodic performance rapidly deteriorated, probably due to the strong cavitation erosion action by a large amount of CO_2 gas from $CaCO_3$ scales formed under -300 mA discharge via HCl, which needs detailed investigation in future. According to the above results, it should be noted that in the application of SWB, not only the MPAN-CFB activity but its long-term stability due to scaling must be considered. Based on the galvanostatic results, a favorable cathodic working current of MPAN-CFB here should be no more than -100 mA.

4 CONCLUSION

After the electrochemical modification, the ORR activity of PAN-CFB was greatly improved. The E_{onset} of MPAN-CFB was positively shifted about 200 mV compared with that of PAN-CFB, and the ORR rate was increased by 6–27 times under different polarization potential. In deep sea, the more seawater flow rate was, the larger ORR rate was, and the increasing tendency slowed down at >3 cm/s. The beneficial dissolved oxygen concentration was >3 mg/L and a low temperature had a negligible effect on ORR rate. A high cathodic working current will form scales on MPAN-CFB surface, resulting in a decrease in ORR activity and the falling of SWB performance. Therefore, to develop a high-performance SWB, it is necessary to improve the activity of cathodic materials, and meanwhile to investigate the working mechanism of marine environmental factors on electrode performance and the scale formation.

5 DATA AVAILABILITY STATEMENT

The data that support the findings of this study are available from the corresponding author upon reasonable request.

References

Barchiche C, Deslouis C, Festy D, Gil O, Refait P, Touzain S, Tribollet B. 2003. Characterization of calcareous deposits in artificial seawater by impedance techniques: 3-Deposit of $CaCO_3$ in the presence of Mg(II). *Electrochimica Acta*, **48**(12): 1 645-1 654.

Chen M. 2009. Chemical Oceanography. Ocean Press, Beijing, China. p.48-102. (in Chinese)

Guo D H, Shibuya R, Akiba C, Saji S, Kondo T, Nakamura J. 2016. Active sites of nitrogen-doped carbon materials for oxygen reduction reaction clarified using model catalysts. *Science*, **351**(6271): 361-365.

Hahn R, Mainert J, Glaw F, Lang K D. 2015. Sea water magnesium fuel cell power supply. *Journal of Power Sources*, **288**: 26-35.

Hasvold Ø. 1990. Seawater batteries for low power, long term applications. *In*: Proceedings of the 34th International Power Sources Symposium. IEEE, Cherry Hill. p.50-52.

Hasvold Ø, Henriksen H, Melv‡r E, Citi G, Johansen B Ø, Kjønigsen T, Galetti R. 1997. Sea-water battery for subsea control systems. *Journal of Power Sources*, **65**(1-2): 253-261.

Hasvold Ø, Lian T, Haakaas E, Størkersen N, Perelman O, Cordier S. 2004. CLIPPER: a long-range, autonomous underwater vehicle using magnesium fuel and oxygen from the sea. *Journal of Power Sources*, **136**(2): 232-239.

Jiao W Q, Fan Y J, Huang C D, Sang L. 2018. Effect of modified polyacrylonitrile-based carbon fiber on the oxygen reduction reactions in seawater batteries. *Ionics*, **24**(1): 285-296.

Liu Q, Wang Y B, Dai L M, Yao J N. 2016. Scalable fabrication of nanoporous carbon fiber films as bifunctional catalytic electrodes for flexible Zn-Air batteries. *Advanced Materials*, **28**(15): 3 000-3 006.

Liu Q F, Yan Z, Wang E D, Wang S L, Sun G Q. 2017. A high-specific-energy magnesium/water battery for full-depth ocean application. *International Journal of Hydrogen Energy*, **42**(36): 23 045-23 053.

Möller H. 2007. The influence of Mg^{2+} on the formation of calcareous deposits on a freely corroding low carbon steel in seawater. *Corrosion Science*, **49**(4): 1 992-2 001.

Morse J W, Arvidson R S, Lüttge A. 2007. Calcium carbonate formation and dissolution. *Chemical Reviews*, **107**(2): 342-381.

Mucci A. 1983. The solubility of calcite and aragonite in seawater at various salinities, temperatures, and one atmosphere total pressure. *American Journal of Science*, **283**(7): 780-799.

Neville A, Morizot A P. 2002. Calcareous scales formed by cathodic protection-an assessment of characteristics and kinetics. *Journal of Crystal Growth*, **243**(3-4): 490-502.

Shinohara M, Araki E, Mochizuki M, Kanazawa T, Suyehiro K. 2009. Practical application of a sea-water battery in deep-sea basin and its performance. *Journal of Power Sources*, **187**(1): 253-260.

Song Y S, Wang S Z. 2004. Research and application of seawater battery. *Torpedo Technology*, **12**(2): 4-8. (in Chinese with English abstract)

Sun L M, Cao D X, Wang G L, Zhang M L. 2008. Metal semi-fuel cells for underwater power source. *Chinese Journal of Power Sources*, **32**(5): 339-342. (in Chinese with English abstract)

Wang Z D, Wang X L, Tian Y. 1997. Seawater aluminum air fuel cell. *Chinese Journal of Power Sources*, **21**(3): 106-109, 113. (in Chinese with English abstract)

Wilcock W S D, Kauffman P C. 1997. Development of a seawater battery for deep-water applications. *Journal of Power Sources*, **66**(1-2): 71-75.

Xu H B, Lu Y H, Zhang W, Yu Y T, Yan C W, Sun Y P, Zhong L, Liu J G, Zheng Y, Han B, Wang Y L. 2012. Dissolved oxygen seawater battery with electrochemical capacitance. *Electrochemistry*, **18**(1): 24-30. (in Chinese with English abstract)

Xu H B, Xia G S, Liu H N, Xia S W, Lu Y H. 2015. Electrochemical activation of commercial polyacrylonitrile-based carbon fiber for the oxygen reduction reaction. *Physical Chemistry Chemical Physics*, **17**(12): 7 707-7 713.

Zha Q X. 2002. Introduction to the Kinetics of Electrode Processes. Science Press, Beijing, China. p.74-122. (in Chinese)